NAS 12-688

The Aluminum Electrode in $AlCl_3$-Alkali-Halide Melts

by

Gerhard L. Holleck and Jose Giner

Tyco Laboratories, Inc.
Bear Hill
Waltham, Massachusetts 02154

ABSTRACT

Passivation Phenomena have been observed upon cathodic and anodic polarization of the Al electrode in $AlCl_3$-KCl-NaCl melts between 100 and 160 °C. They are caused by formation of a solid salt layer at the electrode surface resulting from concentration changes upon current flow. The anodic limiting currents increased with temperature and with decreasing $AlCl_3$ content of the melt. Current voltage curves obtained on a rotating aluminum disk showed a linear relationship between the anodic limiting current and $\omega^{-1/2}$. Upon cathodic polarization dentrite formation occurs at the Al electrode. The activation overvoltage in $AlCl_3$-KCl-NaCl (57.5-12.5-20 mol%) was determined by galvanostatic current step methods. An apparent exchange current density of 270 mA/cm^2 at 130 °C and a double layer capacity of 40 ± 10 μF/cm^2 were measured.

20 pg

Molten salts have been investigated as electrolytes for high energy density batteries. The main disadvantage of the molten electrolyte batteries is the necessity for high temperature operation, which introduces many problems related to materials, construction, safety, etc. Furthermore, the insulation necessary in these high temperature batteries leads to a degradation of their energy density.

In this context, we have carried out studies of a high energy density battery based on an aluminum anode and a chlorine cathode with a molten $AlCl_3$-electrolyte.[1] Aluminum is a low cost readily available material which is easy to handle and has a low equivalent weight. The use of low melting aluminum chloride-alkali-halide mixtures should overcome the problems associated with the high working temperatures of the present molten salt systems, while still retaining the advantages of high energy density and relatively efficient electrode processes. The operating temperature of this system would be in the range of 120-150 °C, with a theoretical energy density of 650 Whr/lb. Furthermore, using an $AlCl_3$-KCl-NaCl eutectic, the battery can be started at 90 °C and the addition of LiCl[2] could reduce the starting temperature to 61 °C.

In this paper, we will discuss the processes occurring at the aluminum electrode in $AlCl_3$-KCl-NaCl melts containing more than 50 mol % $AlCl_3$. The behavior of the chlorine electrode will be discussed elsewhere.[3]

Preparation and Purification of $AlCl_3$-KCl-NaCl Melts

Thermal analysis of the $AlCl_3$-KCl-NaCl system has been carried out by Fischer and Simon[4] and by Midorikawa.[5] The $AlCl_3$-rich region (> 50% $AlCl_3$) constitutes the low temperature region of the phase diagram and is of specific interest for the investigations reported here. Different melting points and compositions have been reported[4-8] for the ternary eutectic ranging from 70 °C for $AlCl_3$-KCl-NaCl (66-14-20 mol %) to 94 °C for $AlCl_3$-KCl-NaCl (62.13, 12.7-25.17 mol %). The most reliable value is probably 89 °C for $AlCl_3$-KCl-NaCl 63.5-16.5-20. Aside from the pseudobinary eutectics $NaAlCl_4$/$AlCl_3$ (108 °C), $KAlCl_4$/$AlCl_3$ (128 °C), and $NaAlCl_4$/$KAlCl_4$ (125 °C), very little is known about the actual phase diagram in this region and about the species present in the melt.

All experimental work was carried out in the argon atmosphere of a purge type glove box. The melts were prepared with Baker "analyzed," KCl and NaCl. In exploratory experiments, $AlCl_3$-KCl-NaCl, 66-14-20 mol % melts were prepared using $AlCl_3$ from eight different manufacturers. Upon heating, greyish brown melts were readily formed. Other investigators[9] have also observed this coloration and attribute it to carbonaceous material and to the presence of $FeCl_3$ impurity in the $AlCl_3$. By investigating the effect of intentional additions of $FeCl_3$, it was confirmed that iron was the major impurity in all melts even where the $AlCl_3$ label stated "iron free."[10] $AlCl_3$ obtained from Fluka Chemicals (Switzerland) was found to contain the lowest impurity level and was thus used as starting material for further purification.

After exploring several purification methods, we settled for the following procedure: A quartz rack containing three electrodes (an Al wire in the center, an Al sheet cylinder as counterelectrodes, and a Pt wire electrode) and a baffle was introduced into a heated 2-ℓ resin reaction kettle, containing a Teflon-coated, magnetic stirring bar. A 1500-g batch of $AlCl_3$-KCl-NaCl (67.5-13.38-19.12 wt %) was introduced into the vessel and heated to 130-140 °C.

At this temperature, the resulting melt had only a moderate $AlCl_3$ vapor pressure.

A high current (~ 10 A) was passed between the Al electrodes with the wire as cathode for several minutes and aluminum dendrites were formed. These dendrites were partially separated from the wire electrode by reversing the current. Thus, clean high surface Al was produced in situ. (We found that, when using Al turnings, the effectiveness of this treatment varied from case to case, probably due to the presence of an aluminum oxide layer.) The melt was kept under constant stirring at 140 °C for 24 to 36 hr.

The progress of the exchange of Fe^{3+} for Al^{3+} was monitored by cyclic potential sweeps at the Pt wire electrode. A reduction in the ionic iron content by more than a factor of 25 was obtained. The temperature was then raised and the $AlCl_3$ evaporated into an aircooled, 1-ℓ reaction kettle placed upside down on top of the reaction vessel. The material so treated was clear and produced virtually transparent eutectics without detectable residual current in the cyclic voltammetric curves obtained on Pt.

The Quasi-Steady State Behavior of the Al Electrode

Experimental: The investigations were carried out at three different $AlCl_3$-KCl-NaCl compositions (melt I: 67-13.6-19.4 mol %; melt II: 59-17-24 mol %; and melt III: 57.5-12.5-30 mol %) and at three different temperatures (157, 126, and 105 °C).

For the measurements on stationary wire electrodes, an electrochemical cell was constructed using two O-ring joints of 50-mm i.d. The electrodes and the gas in and outlet tubes were connected with Teflon Swagelok fittings. The working electrode consisted of a pure Al wire of 1 mm in diameter covered with several layers of shrinkable Teflon tubing except for a length of 1.2 cm. The reference electrode, also an Al wire, was contained in a separate compartment with a narrow opening to protect it from changes in electrolyte concentra-

tion.* An Al wire spiral around the inside of the vessel served as counter-electrode. A platinum electrode sealed into glass was also included in the cell for measurements of the electrolyte background.

A pressure control consisting of an electromagnetic valve and a mercury contact manometer was used to maintain a constant argon pressure (normally, a positive pressure of 10 to 20 torr was used). The cell was filled and assembled tightly in the glove box, then transferred into an air oven (temperature control ±1 °C) and connected to the argon line. No gas was passed through the cell to avoid concentration changes resulting from the appreciable vapor pressure of $AlCl_3$ over the melt. The appearance of the melt was clear, but it turned slightly greyish with time.

The rotating disk assembly and cell are described in detail elsewhere.[3]

Results and Discussion: Melts I and II contained varying amounts of $AlCl_3$ at the KCl/NaCl ratio of the ternary eutectic. The KCl/NaCl ratio in melt III is the same as in the pseudobinary eutectic between $NaAlCl_4$ and $KAlCl_4$. These melts promise to be more favorable for practical application than the composition of the ternary eutectic, since they stay liquid over a wider concentration range at temperatures around 130 °C.

Qualitatively the current voltage curves at an aluminum electrode are very similar in all melts. Typical examples are shown in Figs. 1 through 3. Fig. 4 shows the anodic current as a function of time upon potentiostatic polarization of the Al electrode.

Anodic behavior: The anodic potential sweeps in Figs. 1 through 3 show passivation phenomena. This anodic passivation of the Al electrode does not occur at a constant, defined potential. A closer examination reveals that the sudden current drop can be related to the charge passed (current and time) rather

---

* It had been established[11, 12] that an Al electrode is a stable reference in these melts, and all potentials are referred to this electrode in the particular melt investigated.

Fig. 1. Triangular potential scans at Al electrode, $AlCl_3$-KCl-NaCl (67-13.6-19.4 mol %) 105 °C, 400 mV/min (from 0 mV to E_{cath} to E_{anode} back to 0 mV, no iR correction)

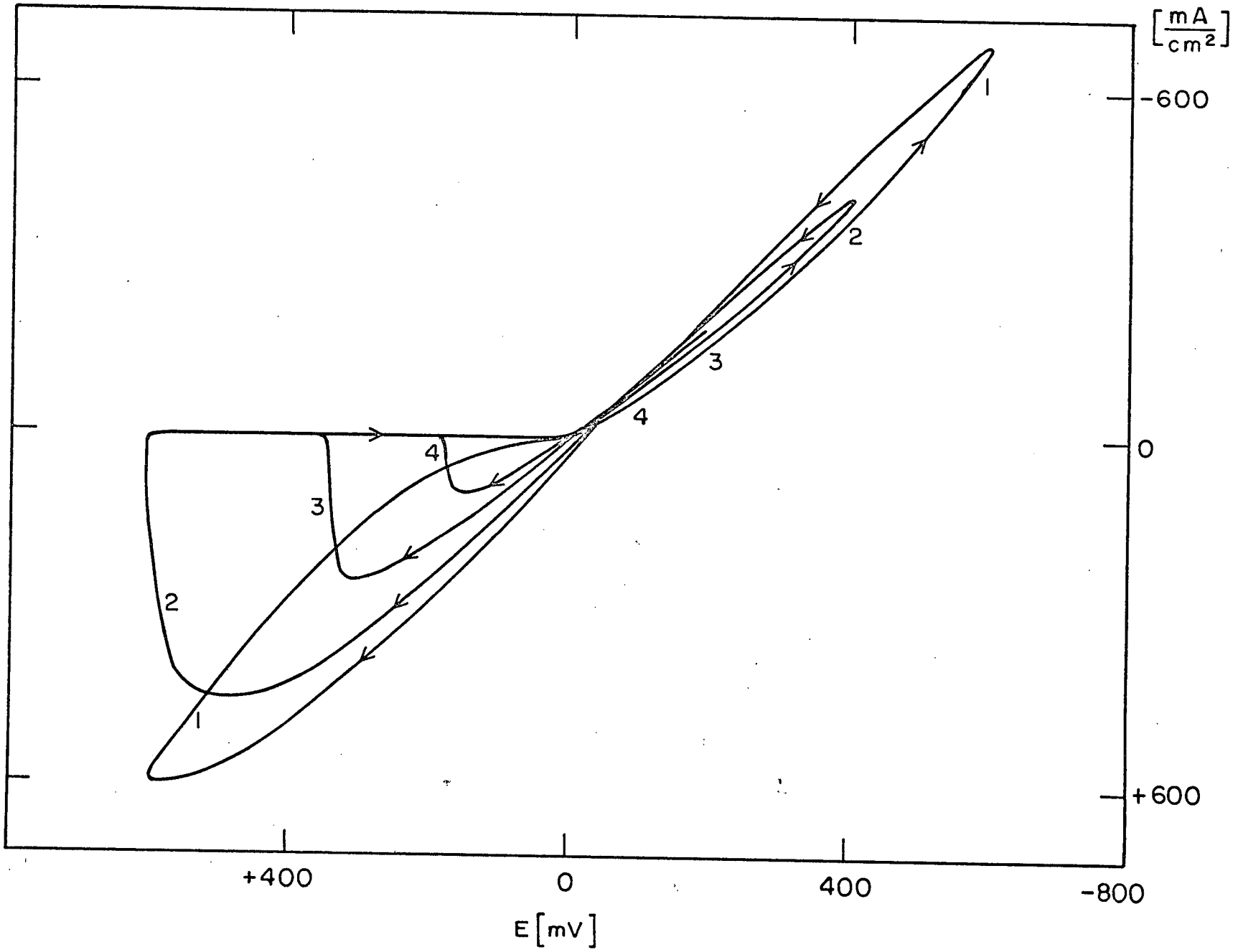

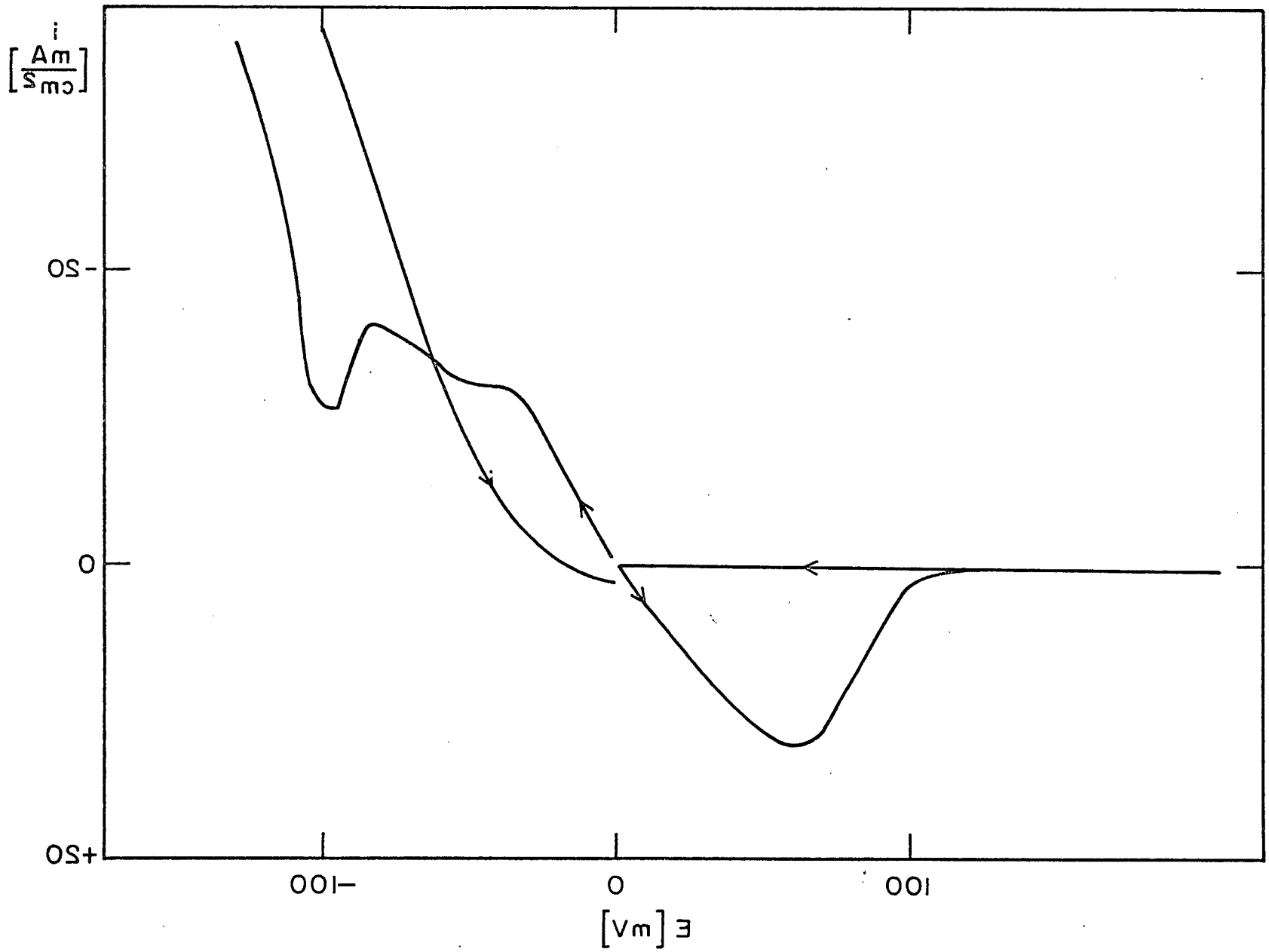

Fig. 2. Separate anodic and cathodic potential scans at an Al electrode. $AlCl_3$-KCl-NaCl (59-77-24 mol %), 105 °C, 20 mV/min (no iR correction)

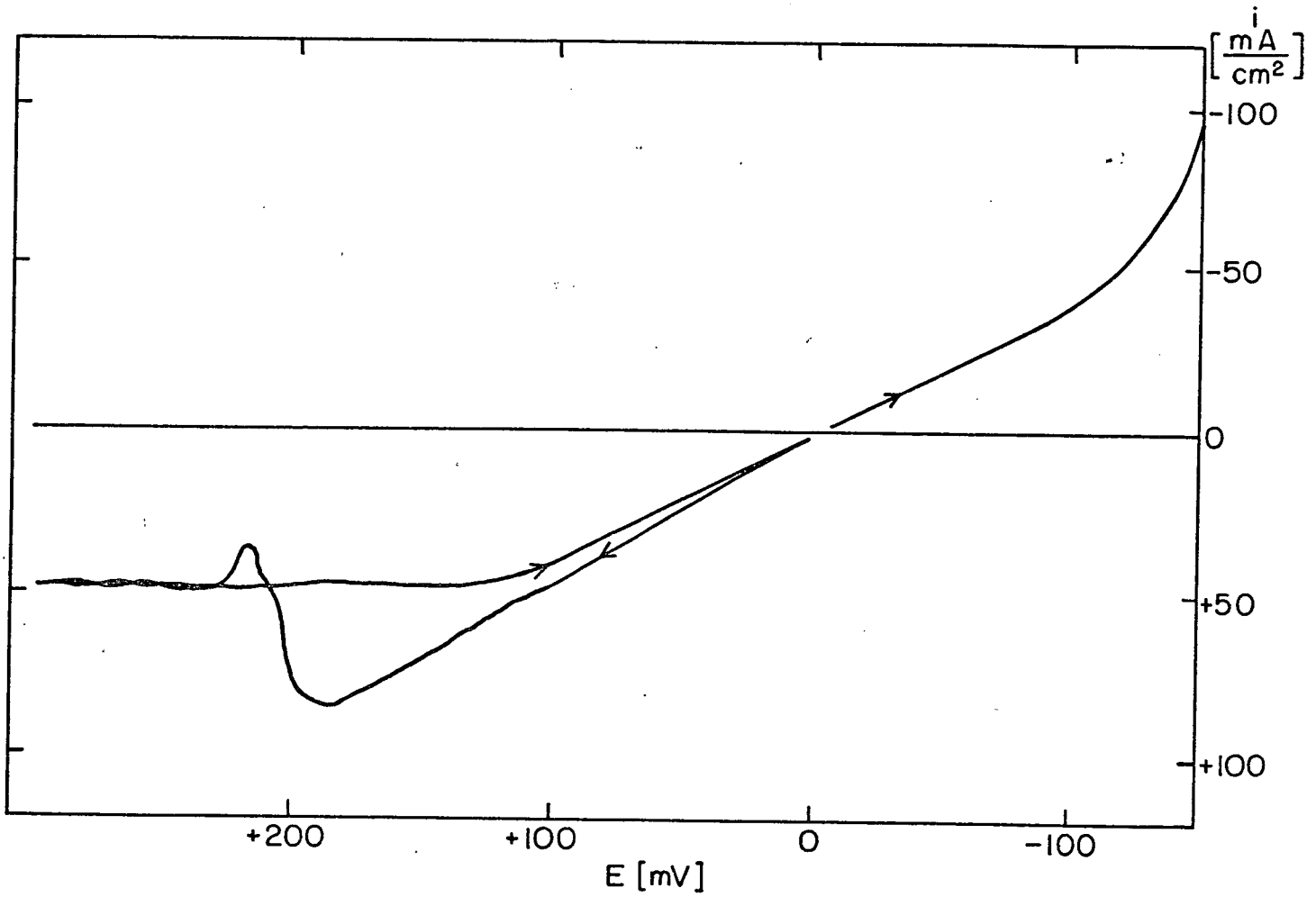

Fig. 3. Separate anodic and cathodic potential scans at an Al electrode. $AlCl_3$-KCl-NaCl (59-17-24 mol %) 157 °C, 20 mV/min, (no iR correction)

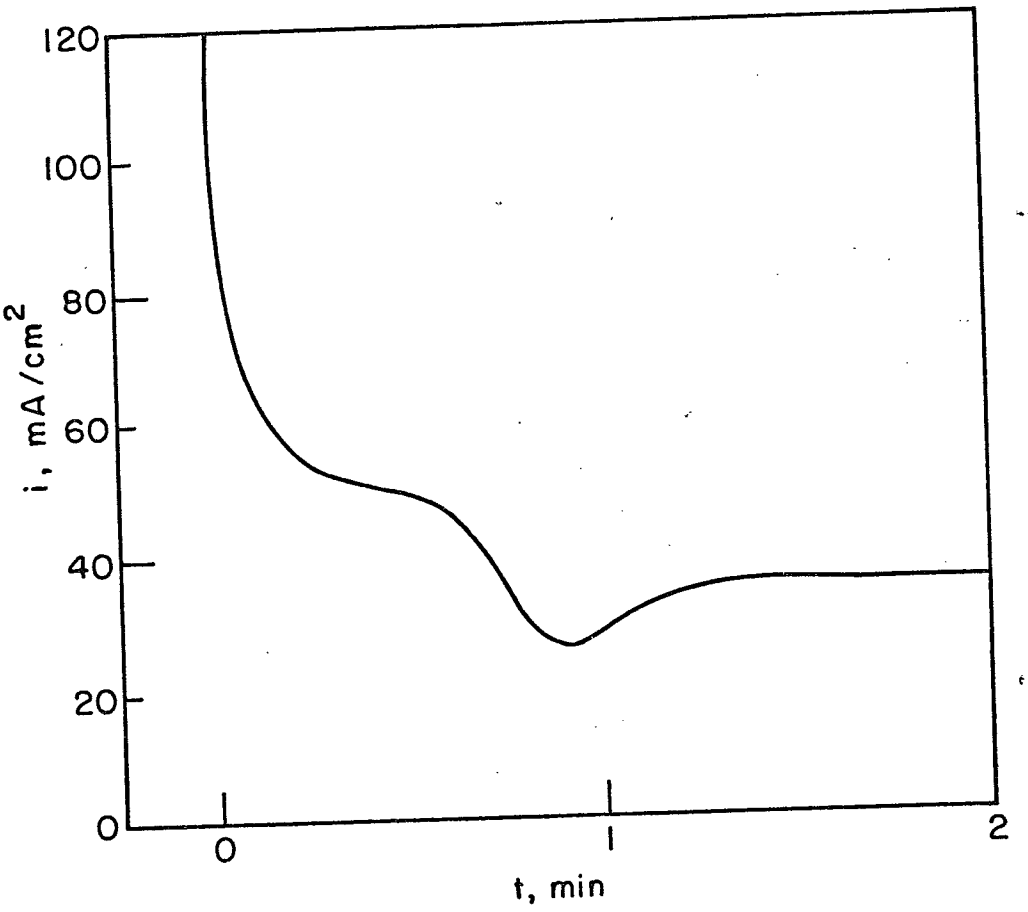

Fig. 4. Anodic current as a function of time upon potentiostatic polarization of Al electrode at 150 mV versus Al in $AlCl_3$-KCl-NaCl (57.5-12.5-30 mol %) at 126 °C (no i-R correction)

than to the potential. Fig. 1 shows the correlation between anodic passivation and cathodic prepolarization for a low temperature with melt I. Comparison of the anodic and cathodic charges (represented by the area underneath the i-t curve) shows that they are nearly equal. This is even more obvious for cathodic and anodic current versus time curves upon potentiostatic polarization for periods of varying length (not shown). This behavior seems to indicate that the melt I (which is $AlCl_3$-rich) cannot tolerate much more anodic formation of $AlCl_3$ at this temperature without precipitating it as an insoluble passivating salt. On the other hand, if by cathodic pretreatment we form a diffusion layer close to the electrode which is poor in $AlCl_3$, then we are able to polarize the electrode anodically for a time necessary to replenish the initial $AlCl_3$ concentration until passivation occurs. Parallel to the current voltage behavior of Fig. 1, it can be seen by microscopic in situ observation of the Al electrode[1] that it is shiny after cathodic polarization, and becomes dull upon passivation. The fact that the anodic and cathodic charges are almost equal indicates a rather compact diffusion layer with practically no convection. As the cathodic prepolarization time is increased, the charge obtained prior to anodic passivation becomes smaller than the cathodic charge, as one would expect.

Cathodic behavior: If the above explanation holds, we should expect a similar passivation effect at cathodic currents due to salt precipitation. In fact, current-voltage sweeps show indications of such a behavior (for example, Fig. 2). In all cases, however, a subsequent current increase is found after indications of passivation. This is due to dendrite formation at the Al electrode. Long, shiny, Al dendrites can easily be seen growing into the electrolyte, thus enlarging the surface area.

The initiation of dendrite growth is a function of current and time. There seems to be a current value below which little dendrite formation is noticeable. This critical current value changes with conditions. Although more detailed

information on the parameters governing dendrite formation is required, our results indicate the strong effect of concentration polarization and ionic conductivity on dendrite formation.

Effect of melt composition: The most obvious difference between the potential scans of the different melts is a much higher, steady state, anodic current after passivation in melts II and III compared to melt I. For example, at 156 °C, the anodic limiting currents are approximately 2 mA/cm^2 for melt I, 50 mA/cm^2 for melt II, and 100 mA/cm^2 for melt III.

On the cathodic side, a deviation from the linear current-potential behavior appears at much larger current densities in melt I than in melt II. This again confirms our explanations of salt formation at the electrode. Melt II, which is less concentrated in $AlCl_3$, can support higher anodic current densities (that means it can accept more Al^{3+} without forming insoluble $AlCl_3$) than melt I. The latter, however, since it is more concentrated in $AlCl_3$, will be able to support higher cathodic currents before forming a passivating salt layer due to X-$AlCl_4$ precipitation (we disregard for the moment the additional complication of dendrite formation). The anodic current maxima (Fig. 3) are very likely due to supersaturation of the melt close to the electrode. After the first crystals have formed, the supersaturation breaks down. This is responsible for the following current dip.

The same effect can be seen in Fig. 4, which shows the anodic current as a function of time upon potentiostatic polarization. Thus, the limiting value of the steady-state current, besides depending on the usual transport properties, also depends on the capacity of the melt to accommodate concentration changes without surpassing the solidus line of the phase diagram. The latter is clearly a function of melt composition.

Effect of temperature: The effect of temperature on the current-voltage behavior of the Al electrode in the molten salt electrolyte can be seen by comparing Figs. 2 and 3, obtained using the same melt. Although a consider-

able steady-state current can be obtained at 157 °C (~ 50 mA/cm^2 in melt II), this steady-state current is practically zero at 105 °C. Melt III shows limiting currents of approximately 100 mA/cm^2 at 157 °C and 34 mA/cm^2 at 126 °C.

The temperature affects the results in several ways. First, there is the temperature dependence of the usual transport phenomena; for example, the viscosity decreases, and the diffusion coefficients increase with rising temperature. Much more important in our case, however, are considerations concerning the $AlCl_3$-KCl-NaCl phase diagram. We mentioned earlier the key role of solid salt formation. How large a concentration change is necessary to surpass the solidus line of the phase diagram is, to a large extent, a function of temperature (besides initial melt composition).

The temperature will surely have an effect on dendrite growth, since this is controlled by diffusion and ohmic polarization. Further changes in conductivity due to varying dissociation constants and changes in complex formation with temperature are to be expected. These problems can, however, not be discussed more closely on the basis of presently available data.

Effect of mass transport: All results of our stationary polarization measurements at Al electrodes indicate that the anodic limiting currents are a function of the mass transport in the melt. We therefore expect the anodic limiting currents to depend on the diffusion layer thickness and thus on the rotation rate of a rotating Al disk electrode. The current which is controlled only by mass transfer is given by Levich:[13]

$$i_L = A \cdot n F D^{2/3} \upsilon^{-1/6} \omega^{1/2} \Delta C$$

where A is a constant, D is the diffusion coefficient, ΔC is the concentration gradient of the electroactive species, υ is the viscosity, and $\omega = 2\pi$ (rps), where rps = rotations per second. This equation implies a linear relationship between i_L and $\omega^{1/2}$ under diffusion controlled conditions.

As Fig. 5 shows, the experimental data can indeed be represented very well by a straight line in such a plot. The slight deviations from linearity and

Fig. 5. Anodic limiting current at rotating Al disk electrode in $AlCl_3$-KCl-NaCl (57.5-12.5-30 mol %) at 125 °C

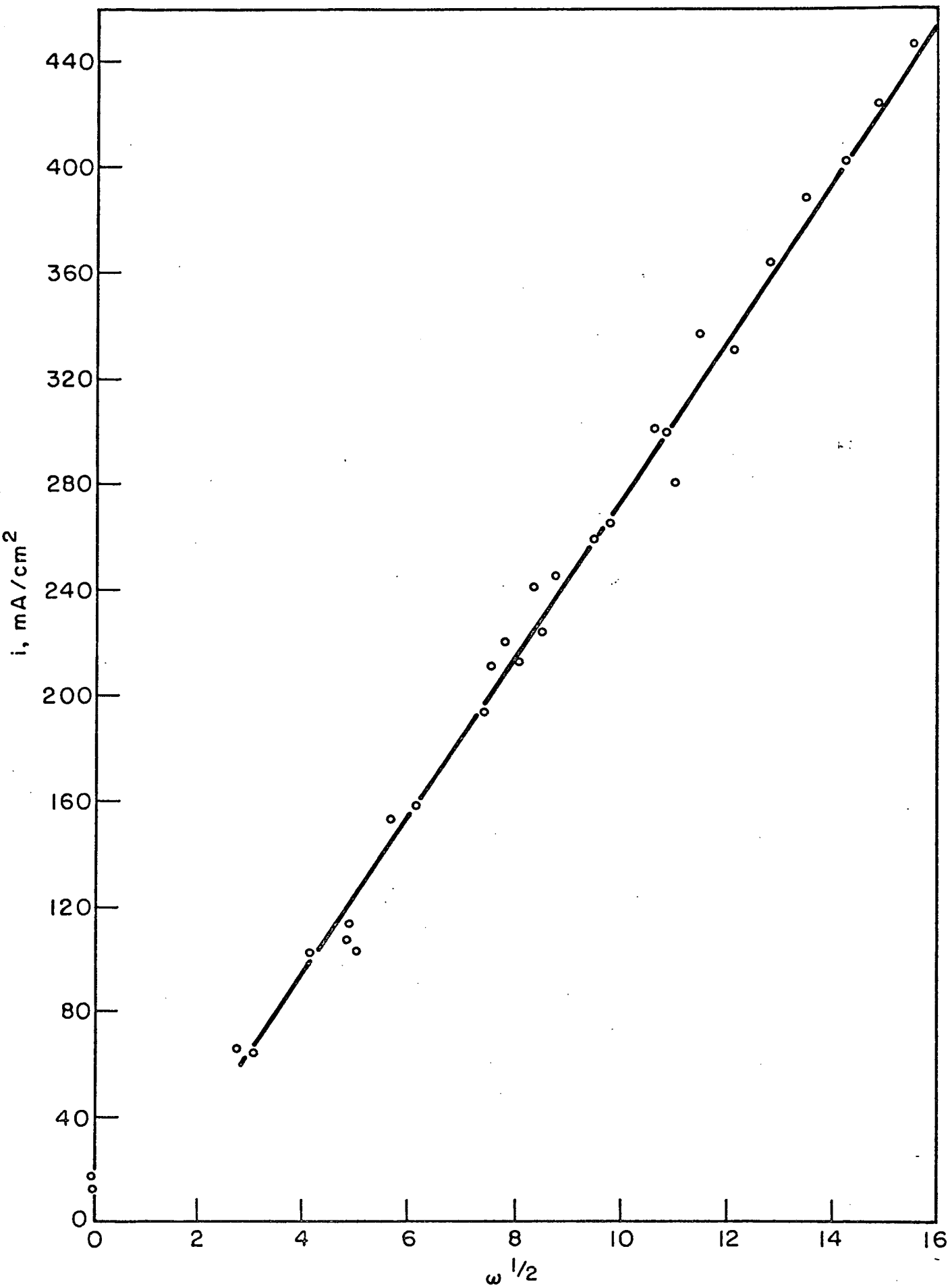

some variations in the individual current densities were to be expected. One must keep in mind that here we are actually dealing with the dissolution of a passivating solid salt layer at the rotating electrode, which is in many respects quite different from the idealized conditions for which the above equation is strictly valid. Further, at the high current densities observed, changes in the electrode itself cannot be avoided.

These results show clearly, however, the role of transport phenomena in removing reaction products from the electrode surface. They show further that high current densities can be obtained at Al electrodes at relatively low temperature if the transport limitations can be overcome.

The Transient Behavior of the Al Electrode

Previous measurements suggested that the charge transfer processes at the Al electrode are quite fast. It is therefore necessary in order to exclude the effect of concentration polarization to use transient methods to investigate the electrode kinetics. We chose galvanostatic pulse measurements for this purpose.

Galvanostatic Current Step Methods: The galvanostatic technique, considering the double layer charging, was originally discussed by Berzins and Delahay[14] and since then, has been used in several investigations.[15] For small overvoltages ($\eta < 0.1$ RT/nF) and for sufficiently long times, the potential transient as a function of a galvanostatic current pulse is given by:

$$\eta = \frac{-2\,RTit^{1/2}}{\pi^{1/2} n^2 F^2 C_o^0 D^{1/2}} + \frac{RTi}{nF}\left[\frac{RTC_{dl}}{n^3 F^3 (C_o^0)^2 D} - \frac{1}{i_o}\right] \qquad (1)$$

Hence, a plot of $\eta/t^{1/2}$ should give a straight line of slope:

$$\frac{d\eta}{d(t^{1/2})} = \frac{-2\,RTi}{\pi^{1/2} n^2 F^2 C_o^0 D^{1/2}} \qquad (2)$$

from which a value for $C_o^0 D^{1/2}$ can be calculated.

When $t^{1/2} = 0$, then

$$\eta = \frac{RTi}{nF}\left[\frac{RTC_{dl}}{n^3F^3(C_o^0)^2D} - \frac{1}{i_o}\right] \tag{3}$$

and the intercept on the η axis, together with the value for $D(C_o^0)^2$ calculated above, will give a value for i_o from Eq. (3).

An alternative method for calculating i_o is the use of a special value of $t^{1/2}$ given by:

$$t_c^{1/2} = \frac{\pi C_{dl}}{4i} \times \frac{d\eta}{d(t^{1/2})} \tag{4}$$

The corresponding overpotential, η_c, can be found from the curve, and a value for i_o calculated.

Both methods require the determination of the differential double layer capacity which can be obtained from the initial slope of the potential time trace at sufficiently short times.[16]

Experimental: In view of the facts mentioned above, it was necessary to use pulses with a short rise time and high current density. It was also necessary to be able to record small potential changes with time, which required a low noise level in the experimental setup and compensation of the ohmic drop in the solution. For the constant current pulses, the output of a Wavetek function generator (gated by a Tyco-built pulse generator to allow multiple pulse application) was used directly. The i-R compensated, potential-time traces were obtained by feeding the potential of the two-electrode cell and the output of the i-R compensation into the inputs of the differential amplifier of a Tektronic dual trace oscilloscope. The measurements were conducted at an Al disk electrode (0.385 cm^2). A sheet of pure Al (15 cm^2) served as the counter-electrode. The experimental setup including the cell showed a response time of about 1 μsec. The melt $AlCl_3$-KCl-NaCl (57.5-12.5-5-30 mol %) was thermo-

stated by a temperature controlled silicone oil bath. Again, a slightly positive argon pressure was kept in the cell at all times.

Results and Discussions: From the initial slope of the potential-time traces at anodic and cathodic current pulses, a double layer capacity of $40 \pm 10\ \mu F/cm^2$ was determined. Considering the surface roughness this suggests the absence of specific absorption effects.

Fig. 6 shows a typical overvoltage versus square root of time plot for various current densities. At times larger than 10 μsec, the potential varies linearily with $t^{1/2}$. As expected, the slope of these lines increases with increasing current density. The times, $t_c^{1/2}$, according to Eq. (4) are also included in Fig. 6. Fig. 7 shows a plot of i versus activation overvoltage. At low overvoltages, one finds a linear relationship between current density and potential. With n = 3, the apparent exchange current at the Al electrode was determined as i_o = 268 mA/cm^2 at 130 °C in the melt $AlCl_3$-KCl-NaCl (57.5-12.5-5-30 mol %).

Schulze and Hoff[17] recently investigated the transference of aluminum in a temperature gradient. From these measurements they deducted similar values for the exchange current at aluminum electrodes in $AlCl_3$-KCl-NaCl (66-14-20 mol %) between 160 and 230 °C [i_o (490 °K) 0.86 A, Q = 9.7 kcal/mol]. They too assume n = 3. Despite reports of multiple electron transfer in molten salts,[18] a three-electron transfer as rate determining step for the aluminum electrode is not established. Thus the available data are not sufficient to decide upon a detailed electrode mechanism. The aluminum electrode has been investigated also in molten $AlCl_3$-NaCl and $AlCl_3$ (LiCl-KCl) by Del Duca.[19] The results are, however, too different in order to allow a meaningful comparison with the present investigation.

Finally, it is interesting to examine more closely the values obtained for the transport parameter, $C_o^0 D^{1/2}$. These values were found to be approximately 1.4×10^{-8}. Assuming a diffusion coefficient of 10^{-6} cm^2/sec in the melt, one obtains for the concentration of the electroactive species $C_o^0 \approx 1.4 \times 10^{-5}$ mol/cm^3. This is about two orders of magnitude less than the excess $AlCl_3$

Fig. 6. Variation of overvoltage with time at Al electrode upon galvanostatic current step in $AlCl_3$-KCl-NaCl (57.5-12.5-30 mol %) at 130 °C

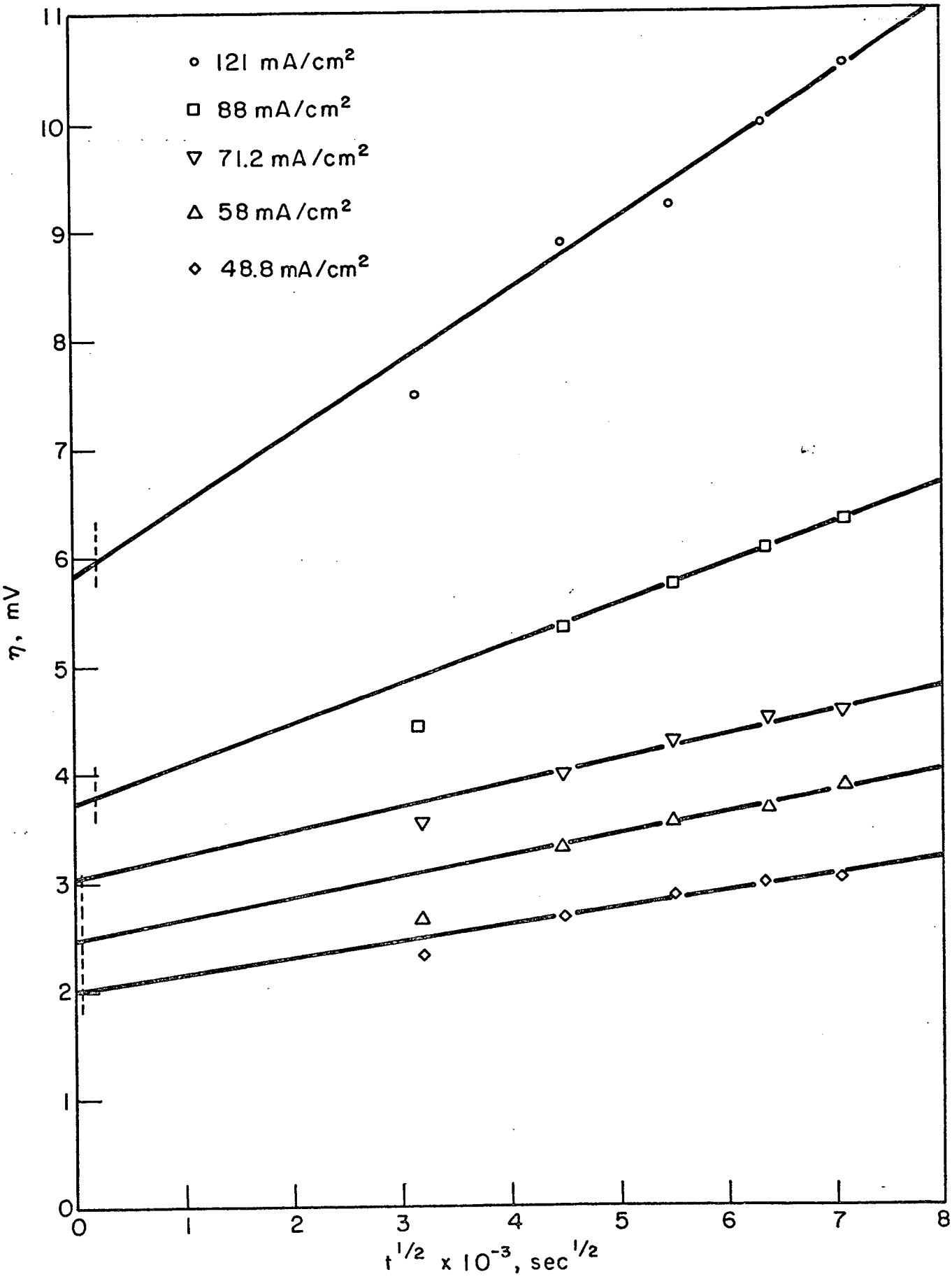

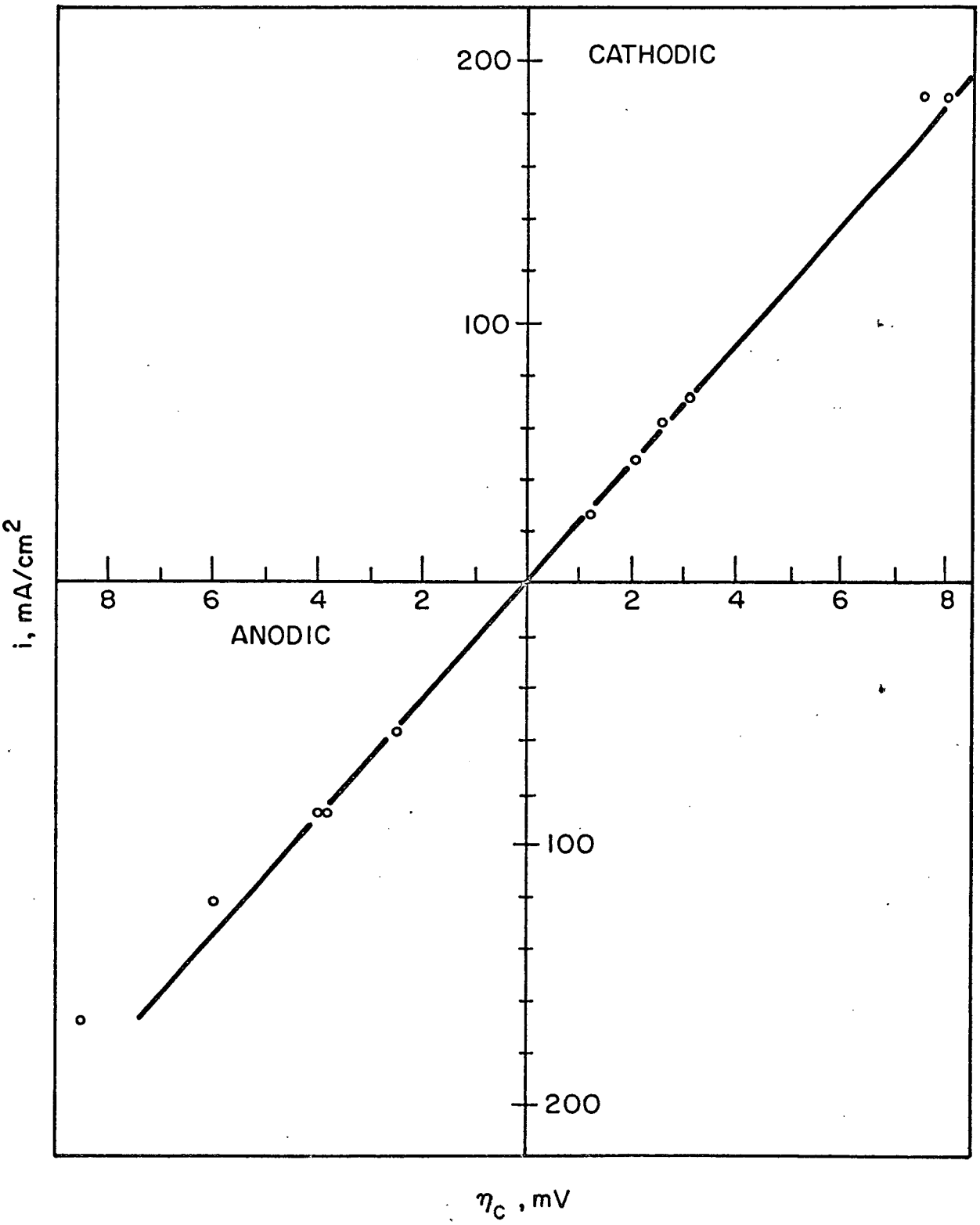

Fig. 7. Current density versus activation overvoltage at Al electrode in $AlCl_3$-KCl-NaCl (57.5-12.5-30 mol %) at 130 °C

assuming 50 mol % $AlCl_3$ to be complexed as $(AlCl_4)^-$. Unfortunately, practically nothing is known about the nature of the species present in the melt and about the complex formation in $AlCl_3$ rich melts.

Conclusions

The behavior discussed above in detail leads us to the following conclusions:

1. The passivation effect is due to the formation of a solid salt layer at the electrode surface caused by concentration changes during current flow.

2. The occurrence of passivation is not dependent on potential, but rather on current and time, i.e., on charge passed through the electrode. It also depends on the transport properties of the melt.

3. The occurrence of salt formation depends on the compositional stability of the melt towards concentration changes. It is strongly dependent on melt composition and on temperature.

4. At cathodic currents, dendrite formation occurs at the Al electrode.

5. The Al electrode itself is highly reversible and able to support large current densities at low activation overvoltage.

6. The polarization observed in the experiments is almost completely ohmic in nature. It again depends on melt composition and temperature.

Acknowledgement

The authors wish to thank Dr. B. Burrows and Mr. M. Turchan for contributions to this investigation. This research was supported by the Electronics Research Center, U. S. National Aeronautics and Space Administration under Contract No. NAS 12-688.

References

1. J. Giner and G. L. Holleck, Final Report by Tyco Laboratories, Inc. on Contract No. NAS 12-688, June 1970.

2. W. E. Trout, Jr. and W. J. Triner, Jr. (University of Richmond) Report No. CCC-1024 TR 139, October 1955.

3. G. L. Holleck, J. Electrochem. Soc., this issue.

4. W. Fischer and A. Simon, Z. Anorg. Allg. Chem., 306, 1-12 (1960).

5. R. Midorikawa, J. Electrochem. Soc., Japan, 23, 127-9 (1955).

6. H. Grothe, Z. Elektrochem., 54, 216-9 (1950).

7. R. Midorikawa, J. Electrochem. Soc., Japan, 23, 352-5 (1955).

8. T. Chao, U. Microfilms, Ann Arbor, Michigan, 3704, 294, Dissertation Abstracts, 12, 459 (1952).

9. T. C. F. Munday and J. D. Corbett, Inorganic Chemistry, 5, 1263 (1966).

10. J. Giner and G. L. Holleck, report prepared under Contract No. NAS 12-688 for National Aeronautics and Space Administration (March 1970). For sale by the Clearinghouse for Federal Scientific and Technical Information, Springfield, Virginia 22151. CFSTI price = $3.00.

11. R. G. Verdieck and L. F. Yntema, J. Phys. Chem., 46, 344 (1942).

12. V. A. Plotnikov, E. J. Kirichenko, and N. S. Fortunatov, Zap. Inst. Khim. Akad. Nauk Ukr. R.S.R., 7, 159 (1945).

13. V. G. Levich, "Physicochemical Hydrodynamics," Prentice Hall, Inc., 1962.

14. T. Bergins and P. Delahay, J. Amer. Chem. Soc., 77, 6448 (1955); Z. Elektrochem., 59, 792 (1955).

15. A. D. Graves, G. J. Hills, and D. Inman, "Advances in Electrochemistry and Electrochemical Engineering," Vol. 4 — Electrode Processes in Molten Salts, P. Delahay, ed., Interscience, 1966.

16. D. Inman, J. O'M. Bockris, and E. Blourgran, J. Electroanal. Chem., 2, 506 (1961).

17. U. Schulze and H. Hoff, Ber. Bunsenges. Physik. Chem., 74, 687 (1970).

18. S. Senderoff and G. W. Mellors, J. Electrochem. Soc., 113, 66 (1966).

19. B. S. Del Duca, J. Electrochem. Soc., 118, 405 (1971).